NASA Technical Memorandum 105985
AIAA–93–0653
ICOMP–92–26

Numerical Simulation of a High Mach Number Jet

M. Ehtesham Hayder and Eli Turkel
Institute for Computational Mechanics in Propulsion
Lewis Research Center
Cleveland, Ohio

and

Reda R. Mankbadi
Lewis Research Center
Cleveland, Ohio

Prepared for the 31st Aerospace Sciences Meeting and Exhibit
sponsored by the American Institute of Aeronautics and Astronautics
Reno, Nevada, January 11–14, 1993

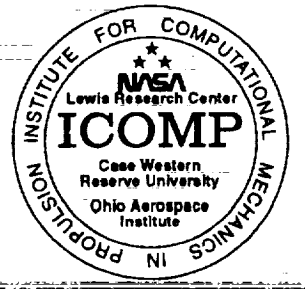

NASA

Numerical Simulations of a High Mach Number Jet Flow

M.E. Hayder, Eli Turkel*
Institute for Computational Mechanics in Propulsion
NASA Lewis Research Center
Cleveland, OH 44135

and
Reda R. Mankbadi**
NASA Lewis Research Center
Cleveland, OH 44135

Abstract

Two dimensional simulations of plane and axisymmetric jets are presented. These simulations were made by solving full Navier-Stokes eqautions using a high order finite difference scheme. Simulation results are in good agreement with the linear theory predictions of the growth of instability waves.

1. Introduction

The recent efforts to develop accurate numerical schemes for transition and turbulent flows are motivated, among other factors, by the need for accurate prediction of flow noise. The success of developing high speed civil transport plane (HSCT) is contingent upon our understanding and suppression of the jet exhaust noise. The radiated sound can be directly obtained by solving the full (time-dependent) compressible Navier-Stokes equations. However, this requires computational storage that is beyond currently available machines. This difficulty can be overcome by limiting the solution domain to the near field where the jet is nonlinear and then use acoustic analogy [e.g., Lighthill[1]] to relate the far-field noise to the near-field sources. The later requires obtaining the time-dependent flow field.

The other difficulty in aeroacoustics computations is that at high Reynolds numbers the turbulent flow has a large range of scales. Direct numerical simulations (DNS) cannot obtain all the scales of motion at high Reynolds number of technological interest. However, it is believed that the large scale structure is more efficient than the small-scale structure in radiating noise [see, e.g., Bishop et. al[2], Crington[3], Goldstein[4], Hussain[5,6], Kibens[7], Liu[8,9], Mankbadi and Liu[10], Mankbadi[11,12], Mollo-Christensen[13], and Zaman[14,15]]. Thus, one can model the small scales and calculate the acoustically active scales. The large scale structure in the noise-producing initial region of the jet can be viewed as a wavelike nature, the net radiated sound is the net cancellation after integration over space. As such, aeroacoustics computations are highly sensitive to errors in computing the sound sources. It is therefore essential to use a high-order numerical scheme to predict the flow field.

The present paper presents the first step in a ongoing effort to predict jet noise. The emphasis here is in accurate prediction of the unsteady flow field. We solve the full time-dependent Navier-Stokes equations by a high order finite difference method. Time accurate spatial simulations of both plane and axisymmetric jet are presented. Jet Mach numbers of 1.5 and 2.1 are considered. Reynolds number in the simulations was about a million. Our numerical model is based on the 2-4 scheme by Gottlieb & Turkel[16,17]. Bayliss et al.[18] applied the 2-4 scheme in boundary layer computations. This

* Also Department of Mathematics, Tel Aviv University.

** Associate Fellow AIAA

scheme was also used by Ragab and Sheen[19] to study the nonlinear development of supersonic instability waves in a mixing layer.

In this study, we present two dimensional direct simulation results for both plane and axisymmetric jets. These results are compared with linear theory predictions. These computations were made for near nozzle exit region and velocity in spanwise/azimuthal direction was assumed to be zero. Computational domain of the present study is shown in Figure 1.

2. Governing Equations

The flow field of the technologically important high-Reynolds-number compressible jet is governed by the compressible Navier-Stokes equations, which can be written as

$$LQ = 0 \tag{1}$$

Where L is a three-dimensional operator and Q is the solution vector. Here we present the two dimensional form of the operator L pertaining to our formulations in the polar coordinates.

$$\frac{\partial Q}{\partial t} + \frac{\partial F}{\partial x} + \frac{\partial G}{\partial r} = S \tag{2}$$

where

$$Q = r \begin{pmatrix} \rho \\ \rho u \\ \rho v \\ \rho E \end{pmatrix} \tag{3}$$

$$F = r \begin{pmatrix} \rho v \\ \rho u^2 - \tau_{xx} + p \\ \rho uv - \tau_{xr} \\ \rho uH - u\tau_{xx} - v\tau_{xr} - \kappa T_x \end{pmatrix} \tag{4}$$

$$G = r \begin{pmatrix} \rho u \\ \rho uv - \tau_{xr} \\ \rho v^2 - \tau_{rr} + p \\ \rho vH - u\tau_{xr} - v\tau_{rr} - \kappa T_r \end{pmatrix} \tag{5}$$

$$S = \begin{pmatrix} 0 \\ 0 \\ p - \tau_{\theta\theta} \\ 0 \\ 0 \end{pmatrix} \tag{7}$$

F and G are the fluxes in x and r directions respectively, and S is the source term that arises in the cylindrical polar coordinates, and τ_{ij} are shear stresses.

3. Numerical Scheme

3.1 Discretization

For problems in computational acoustics one needs to use high order (at least fourth order) schemes. Hence, in this study, Gottlieb and Turkel's extension[16,17] of MacCormack's scheme is used. The extension is fourth-order accurate in space and second order accurate in time and is known as the 2-4 scheme. For three dimensional computations, operator L in equation (1) is split into three one-dimensional operators and the 2-4 scheme is applied to each of the three operators as

Predictor step

$$\bar{Q}_i = Q_i^n + \frac{\Delta t}{6\Delta x}\{7(F_{i+1}^n - F_i^n) - (F_{i+2}^n - F_{i+1}^n)\} + \Delta t S_i \tag{8}$$

Corrector step

$$Q_i^{n+1} = \frac{1}{2}[\bar{Q}_i + Q_i^n + \frac{\Delta t}{6\Delta x}\{7(\bar{F}_i^n - \bar{F}_{i-1}^n) - (\bar{F}_{i-1}^n - \bar{F}_{i-2}^n)\} + \Delta t S_i] \tag{9}$$

This scheme becomes fourth-order accurate in the spatial derivatives when alternated with symmetric variants. We define L_1 as an one dimensional 2-4 scheme operator with forward difference in the predictor and backward difference in corrector. Its symmetric variant L_2 uses backward difference in predictor and forward difference in the corrector.

For two dimensional computations, one dimensional sweeps are arranged with alternate symmetric variants as

$$Q^{n+1} = L_{1x}L_{1r}Q^n \tag{10.1}$$

$$Q^{n+2} = L_{2r}L_{2x}Q^{n+1} \tag{10.2}$$

Our scheme has a truncation error of the form $O(\Delta t((\Delta x)^4 + (\Delta t)^2 + (\Delta t)(\Delta x)^2))$. For $\Delta t = O((\Delta x)^2)$ as $\Delta x \to 0$, this scheme becomes fourth order accurate.

3.2 Boundary Conditions

The 2-4 scheme uses one sided differences of the fluxes. For a computational domain extending from i=1 to m, fluxes are needed at m+1,

m+2, -2, -1 in addition to the interior points. The fluxes at points outside the computational domain are estimated using cubic extrapolation from the interior, i.e.,

$$F_{m+1} = 4F_m - 6F_{m-1} + 4F_{m-2} - F_{m-3} \quad (11.1)$$

$$F_{m+2} = 4F_{m+1} - 6F_m + 4F_{m-1} - F_{m-2} \quad (11.2)$$

At the centerline, a new set of equations are derived from the original equations using L'Hospitals rule to circumvent numerical problems associated with geometric singularity in the formulation.

Physical boundary conditions for the computations are derived using linearized characteristics. For supersonic flows, all characteristics travel in the flow direction. At inflow all variables are given. For outflow, the variables are calculated applying the 2-4 scheme at the boundary. Extrapolations of variables outside the domain are done using equation (11). We stress that extrapolation of fluxes to artificial points is identical to using one sided differences. The extrapolation is used for programming convenience only. For subsonic flows, one characteristic variable propagates against the flow direction while the rest follow the flow direction. For inflow, three characteristic variables are specified and the other one is extrapolated from interior. We formulated our outflow boundary conditions following the results of Bayliss and Turkel[20]. In particular, we solve equation (12) to predict the flow variable at the boundaries.

$$P_t - \rho c u_t = \gamma_1 \quad (12.1)$$

$$P_t + \rho c u_t = \gamma_2 \quad (12.2)$$

$$P_t - c^2 \rho_t = \gamma_3 \quad (12.3)$$

$$v_t = \gamma_4 \quad (12.4)$$

The derivatives of P, u, v, ρ are then converted to derivatives of the conservative variables. The right hand side of the above equations are calculated from the solution obtained by applying the 2-4 scheme at the boundaries. If the flow at a point at the outflow boundary is subsonic, γ_1 is set to zero. If the flow at the boundary is supersonic, the value of γ_1 is kept unchanged. Equation (12) is then solved to get corrected temporal derivatives at the boundary. Thus, for supersonic flow (12) is equivalent to using the PDE at the outflow with one sided differences. For subsonic flow a nonreflecting boundary condition is used. In a future paper several nonreflecting boundary conditions will be compared. These all are included in generalizations of (12.1). We obtained the present form of (12.1) by simplifying the Bayliss-Turkel formulation[20] and neglecting spatial derivatives. Flow at the top boundary is always subsonic and a similar characteristic boundary condition is applied.

4. Results

In this study, our primary goal is to simulate aerodynamic noise associated with a supersonic jet flowing into a subsonic free stream. In the short term, we are interested in computing growth rates of the disturbances imposed at the inflow. These computations are done in two stages, (a) first a mean (steady) state of the field with steady inflow condition is obtained and then (b) transient behavior of the flow with periodic excitations at the inflow is calculated.

For the mean state calculations, we start with an initial field which is homogeneous in the axial direction. The initial axial velocity is specified as

$$\bar{u}(y) = \frac{1}{2}[(1+u_\infty) - (1-u_\infty) \tanh(a(y-y_1))] \quad (13)$$

and corresponding temperature is specified by the Busemann-Crocco integral of energy equation as

$$T(y) = T_\infty + (T_0 - T_\infty)(\bar{u} - u_\infty)/(1-u_\infty) + .5(\gamma-1)M^2(1-\bar{u})(\bar{u}-u_\infty) \quad (14)$$

The parameter "a" in the equation (13) determines the sharpness of the velocity profile. The axial velocity is normalized by its initial value at the center of the jet. At location y_1 at the inflow plane, axial velocity is the average of the jet center and free stream value. Throughout the whole simulation, variables at the boundary, including those at the inflow are updated using characteristics boundary condition described in § 3.2. We assume Prandlt number to be 1, and

the kinematic viscosity is calculated using Sutherland law. The initial static pressure is assumed uniform across the field and density is calculated from the equation of the state. Initial radial/transverse velocity in the field is set to be zero.

Once the steady state of the field is reached, a time varying disturbance is applied at the inflow. In our present study, only the axial velocity is perturbed. It is done by prescribing the axial velocity at the inflow as

$$u(y,t) = \bar{u}(y)(1 + \epsilon\ sin(\omega t)) \qquad (14)$$

Other variables at the inflow are kept at their steady state values. Depending on the value of the forcing frequency (ω), input disturbance undergoes either amplification or decay. For an amplifying disturbance, the initially growth is linear. However, as the amplitude of the disturbance grow, the process becomes nonlinear and disturbances with other frequencies appear in the field. Smaller values of ϵ delays the appearance of nonlinear effects downstream. Corresponding to a forcing frequency (ω) of the input disturbances, there are some disturbance eigenfunctions (Φ_ω) of the flow variables. Disturbances with shapes of the eigenfunction exhibit dominant growth. The shape of the disturbance as given in equation (14), is different from those of the eigenfunctions. With our choice of input disturbance, we left the simulation to generate the correct mode shape of the instability eigenfunctions. Study of instability mode growth with input disturbances as eigenfunction shapes in all the variables are in progress. In the following we present simulation results in this study.

4.1 Plane Jet

A case of a coflowing plane jet is considered first. The jet Mach number, based on axial velocity at the center of jet was 1.5, velocity ratio (u_∞/u_0) and temperature ratio (T_∞/T_0) were .74 and 2 respectively. This combination made Mach number at the free stream about the half of the jet Mach number. Parameter "a" [equation (13)] in the initial axial velocity profile was 4. The computational domain extended 50 jet thickness in the downstream direction and 2.5 jet thickness in the transverse direction. We used 600 mesh points in axial and 60 mesh points in transverse direction. The mesh was uniform in axial and stretched in transverse direction. Reynolds number based on the jet thickness and the inlet axial velocity was 1.27 million.

4.1.1 steady state simulation

Parameters for our simulation were chosen to given very small spreading of the jet. This condition is ideal for comparison of the simulation results with weakly nonparallel linear theory. Profiles of axial velocities at three downstream locations are shown in Figure 2. These velocities were computed after the steady state was reached. Differences in these profiles are insignificant. Contour plots of steady state vorticity and axial velocity for the whole domain is shown in Figure 3. The y axis in these figure is magnified to show the the whole domain. The flow remains virtually parallel and spreading of the jet or any tread towards the formation of the potential core is not noticeable. If the flow is not well resolved, numerical (truncation) errors inject disturbances in the flow and that in turn could give rise to different flow structures in the solution. Our choice of grid results in well resolved flow for the present study. Small linear growth of both momentum and vorticity thicknesses was observed in the steady state flow field. Vorticity thickness as defined by

$$\delta_v = (U_0 - U_\infty)/(du/dy)_{max}$$

varied between .5 and .505. Also, momentum thickness defined as

$$\delta_m = \int \frac{\rho(U_0 - U)(U - U_\infty)}{(U_0 - U_\infty)^2} dy$$

varied between .086 and .087. Once the steady state solution is established, we concentrate on the unsteady state simulation.

4.1.1 Time dependent simulation

Now we shall discuss results of a time dependent simulation with periodic disturbance for $\omega = \pi/5$ and $\epsilon = .001$. Contour plots of vorticity and axial velocity are shown in Figure 4. Input disturbance grows spatially and causes vorticities to form. These structures becomes prominent downstream. Near the outflow, the input disturbance reached its maximum strength and made the flow to oscillate. Care should be taken in boundary treatment, since numerical reflections at the boundary also contribute to such oscillations.

Figure 5 shows mean axial velocities at three downstream locations. These were obtained by

computing the zeroth Fourier mode of the unsteady axial velocity. As expected, mean axial velocity remained at their steady state values. After long time, the flow field became spatially nonhomogeneous but time periodic about its steady state. Since the shape of the inflow perturbation did not correspond to any eigenfunction of instability wave, the flow underwent an adjustment region where the simulation picked up the correct mode shape of instability waves downstream. In Figure 6 the mode shape of the eigenfunction (Φ) corresponding to the forcing frequency (ω) at two downstream locations are compared with the linear theory prediction. Mode shapes form the direct numerical simulations are obtained by taking Fourier transform in time. As expected, DNS prediction of these shapes improved as the flow moved away from the inlet region. There is, however, a small phase shift between the DNS prediction and the linear theory predictions. In Figure 7, we examine the growth of the instability mode (Φ_ω) corresponding to the forcing frequency, whose shape is given in Figure 6. For the DNS, growth rate is calculated along y=y_1 line. At this vertical location, the shear in the mean axial velocity profile is the highest. There is a good agreement between the simulation and the linear theory. DNS predictions differ from the linear theory predictions near outflow. This may be due to excitation of instability waves at other frequencies or non-linear effects in the flow. Growth rate (-α_i) predicted by both the linear theory and DNS at X =50 is .054. As the disturbances grow spatially downstream, non-linear effects excited other instability modes. Two such modes for the simulation are shown in Figure 8. For our simulation, any such mode was significant only near the outflow boundary.

Simulations were also performed for Jet Mach number 2.1 and higher velocity ratios. Comparisons of one such simulation results with the linear theory are shown in Figures 9 & 10. Velocity and temperature ratios were .2 and 1 respectively. Parameter "a" in the initial axial velocity profile was 6. Computational domain extended 35 jet thickness downstream and 2.5 jet thickness in the transverse direction. Mesh size in the axial and the transverse directions were 400 and 150, and stretching was used in both directions. For the unsteady calculations, we used $\omega = \pi/8$ and $\epsilon = 10^{-5}$.

4.1 Axisymmetric Jet

Results of the axisymmetric jet simulations are similar to those in the plane jet case. Here we present results of an axisymmetric jet simulation with Mach number 1.5 in the jet, velocity ratio $(u_\infty/u_0) = .75$ and temperature ratio $(T_\infty/T_0) = 2$. "a" in the axial velocity profile equation was 4. The computation domain extended 100 radii downstream and 5 radii in radial direction. 400 grid points were used in axial and 100 grid points were used in radial direction. The grid spacing was uniform in axial and stretched in radial direction. The Reynolds number of this flow was the same as in plane jet case.

4.1.1 steady state simulation

Contour plot of the vorticity for the steady state simulation is shown in Figure 11. The Y (radial) axis in these figures is magnified to show the whole computational domain. As in the case of plane jet, in steady state simulation, the flow remained virtually parallel.

4.1.1 Time dependent simulation

A time dependent simulation with $\omega = \pi/4$ and $\epsilon = .005$ was made to study the growth of disturbance mode. Contour plots of vorticity and axial velocity of the time dependent field are shown in Figure 12. These plots show spatial growth of oscillatory flow structures caused by instability modes. Growth of disturbance corresponding to the forcing mode is compared with the linear theory predictions in Figure 13. Agreement between the linear theory and DNS predictions are similar to those in plane jet case. Small discrepancy between linear theory and DNS near inlet is likely due to the fact that the flow underwent an adjustment region, because the input disturbance did not have correct shape of an instability eigenfunction. Discrepancy near outflow region are likely because of the similar reasons as in plane jet case. Growth rate (-α_i) predicted by both the linear theory and DNS at X =50 is .035. Comparison of mode shape as predicted by the linear theory and DNS simulations at 50 radii downstream is given in Figure 14. Except close to the center of the jet, DNS prediction of the mode shape is in good agreement with the linear theory. Excitation of two modes due to nonlinear effects are shown in Figure 15. DNS results in Figures 14 & 15 are obtained exactly as their counterparts in plane jet simulations.

5. Conclusions

In this study, we have presented a set of Navier Stokes simulations for both two dimensional plane and axisymmetric jets. Parameters were so chosen to give almost parallel mean flow. This enabled us to compare our results with weakly nonparallel linear theory. Agreement with the linear theory are quite good. We imposed time periodic disturbances which did not correspond to the instability eigenfunction shape. Nevertheless, the simulation was able to generate the correct mode shape after an adjustment region ($\sim$ 10 diameters) and comparison with linear theory afterward is good.

The boundary condition is very important for jet simulation. We formulated the outflow boundary condition by simplifying the Bayliss-Turkel[20] nonreflecting boundary condition. Efforts to improve the outflow boundary condition are in progress.

Acknowledgements

The linear stability -theory results were obtained using a code developed by Dr. Lennart S. Hultgen. We gratefully acknowledge his help using the code.

References

[1]Lighthill, M. J., (1952), "On Sound Generated Aerodynamically, Part I, General Theory", *Proc. Roy. Soc. London,* Vol 211, pp 564-587.

[2]Bishop, K. A., Ffowcs-Williams, J. E., and Smith, W. (1971), "On the Noise source of Unsuppressed High Speed Jet", *J. Fluid Mech,* Vol 50, pp 21-31.

[3]Crighton, D.G. (1981). "Acoustics as a Branch of Fluid Mechanics", *J. Fluid Mech,* Vol 106, pp 261-298.

[4]Goldstein, M.E. (1984) "The Aeroacoustics of Turbulent Shear Flows", *Annual Review of Fluid Mechanics.*

[5]Hussain, A. K. M. F., (1983), "Coherent Structures – Reality and Myth", *Physics of Fluids,* Vol 26, pp 2816-28.

[6]Hussain, A. K. M. F., (1986), "Coherent Structures and Turbulence", *J. Fluid Mech.,* vol 173, pp 303-356.

[7]Kibens, V., (1980), "Discrete Noise Spectrum Generated by an Acoustically Excited Jet", *AIAA J.,* Vol 18, pp434-441.

[8]Liu. J.T.C., (1971), "Nonlinear Development of an Instability Wave in a Turbulent Wake", *Phys of Fluids,* Vol 14, pp 2251-2257.

[9]Liu, J.T.C., (1974), "Developing Large-Scale Wavelike Eddied and the Near Jet Noise Field", *J. Fluid Mech.,* Vol 62, pp 437-464.

[10]Mollo-Christensen, E., (1967),"Jet Noise and Shear Flow Instability Seen from an Experimental Viewpoint", *J. Appl. Mech.,* Vol 89, pp 1-7.

[11]Zaman, K. B. M. Q., (1985), "Far-Field Noise of a Subsonic Jet Under Controlled Excitation", *J. Fluid Mechanics,* Vol 152, pp83-112.

[12]Zaman, K. B. M. Q., (1986), "Flow Field and Near and Far Sound Field of a Subsonic Jet", *J. Sound and Vibration,* Vol 106, pp 1-6.

[13]Mankbadi, R. R. and Liu J.T.C, (1984), "Sound generated Aerodynamically Revisited: Large-scale Structures in a Turbulent Jet as a Source of Sound", *Phi Trans Roy Soc London,* A, Vol 311, pp 183-217.

[14]Mankbadi, R. R., (1990), " The Self Noise from Ordered Structures in a Low Mach Number Jet", *J Appl Mech* Vol 57, pp 241-246.

[15]Mankbadi, R. R. (1992), "Dynamics and Control of Coherent Structure in Turbulent Jets", *Appl Mech Rev,* Vol 45, No 6, pp 219-248.

[16]Gottlieb, D. and Turkel, E. (1976), "Dissipative Two-Four Methods for Time Dependent Problems", *Math. Comp,* Vol 30, pp 703-723.

[17]Bayliss, A., Paresh, P., Mastrello, L., and Turkel, E., (1985), "A Fourth-order Scheme for Unsteady Compressible Navier-Stokes Equations", ICASE report 85-44.

[18]Bayliss, A., Maestrello, L. A., Parikh, P. and Turkel, E. (1986), "Numerical Simulation of Boundary Layer Excitation by Surface Heating and Cooling", *AIAA J.,* Vol 24, pp 1095-1101.

[19]Ragab, S. A. and Sheen, S. (1992), "The Nonlinear Development of Supersonic Instability Waves in a Mixing Layer", *Phys. Fluids A* Vol 4(3),pp 553-566.

[20]Bayliss, A. and Turkel, E., (1982), "Far Field Boundary Condition for Compressible Flows", *Journal of computational Physics,* Vol 48, pp 182-199.

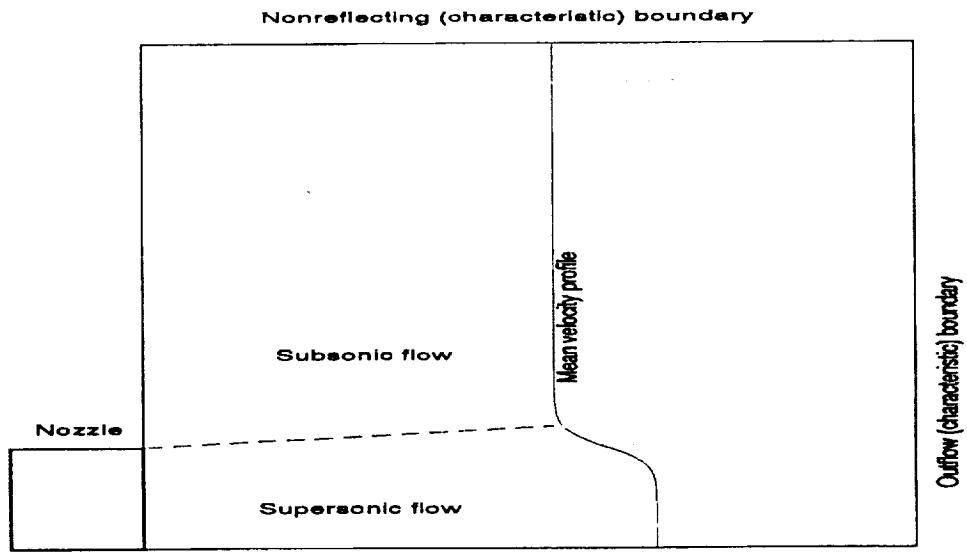

Fig 1: Computational Domain

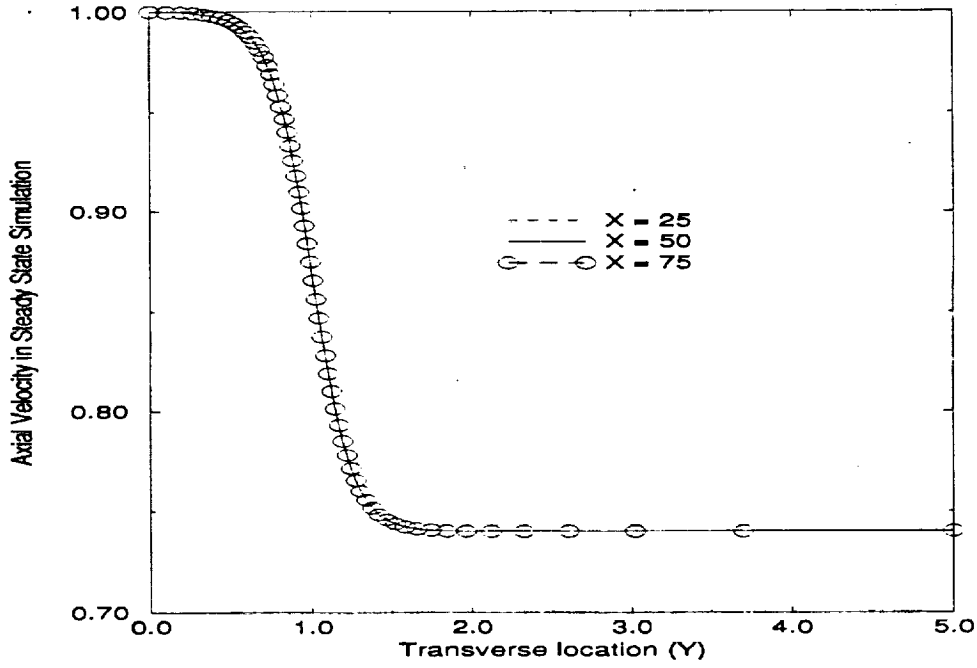

Figure 2: Axial velocity profile in Plane Jet

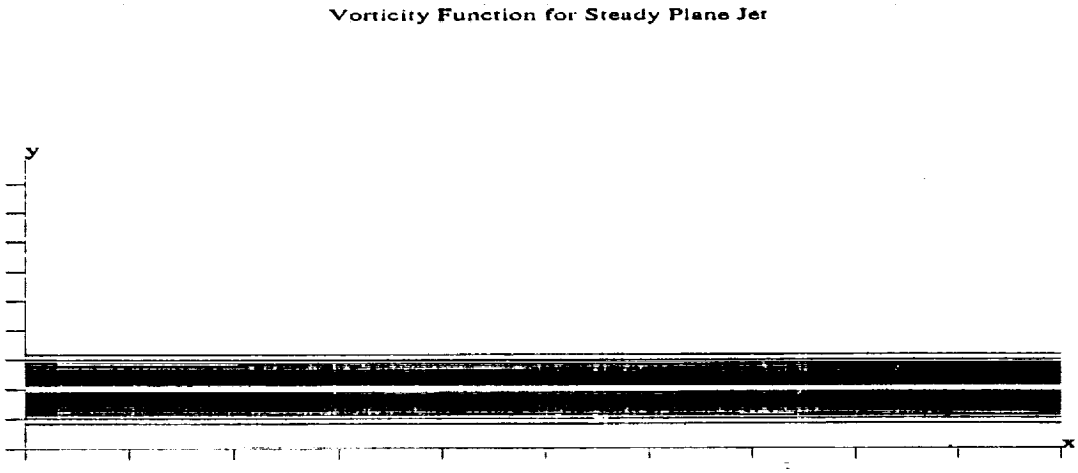

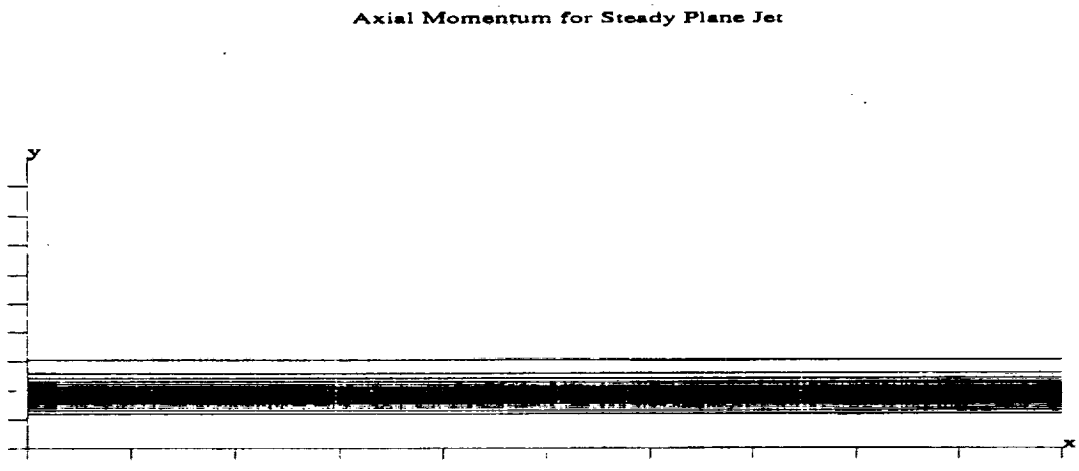

Figure 3: Contour Plots for Steady Plane Jet

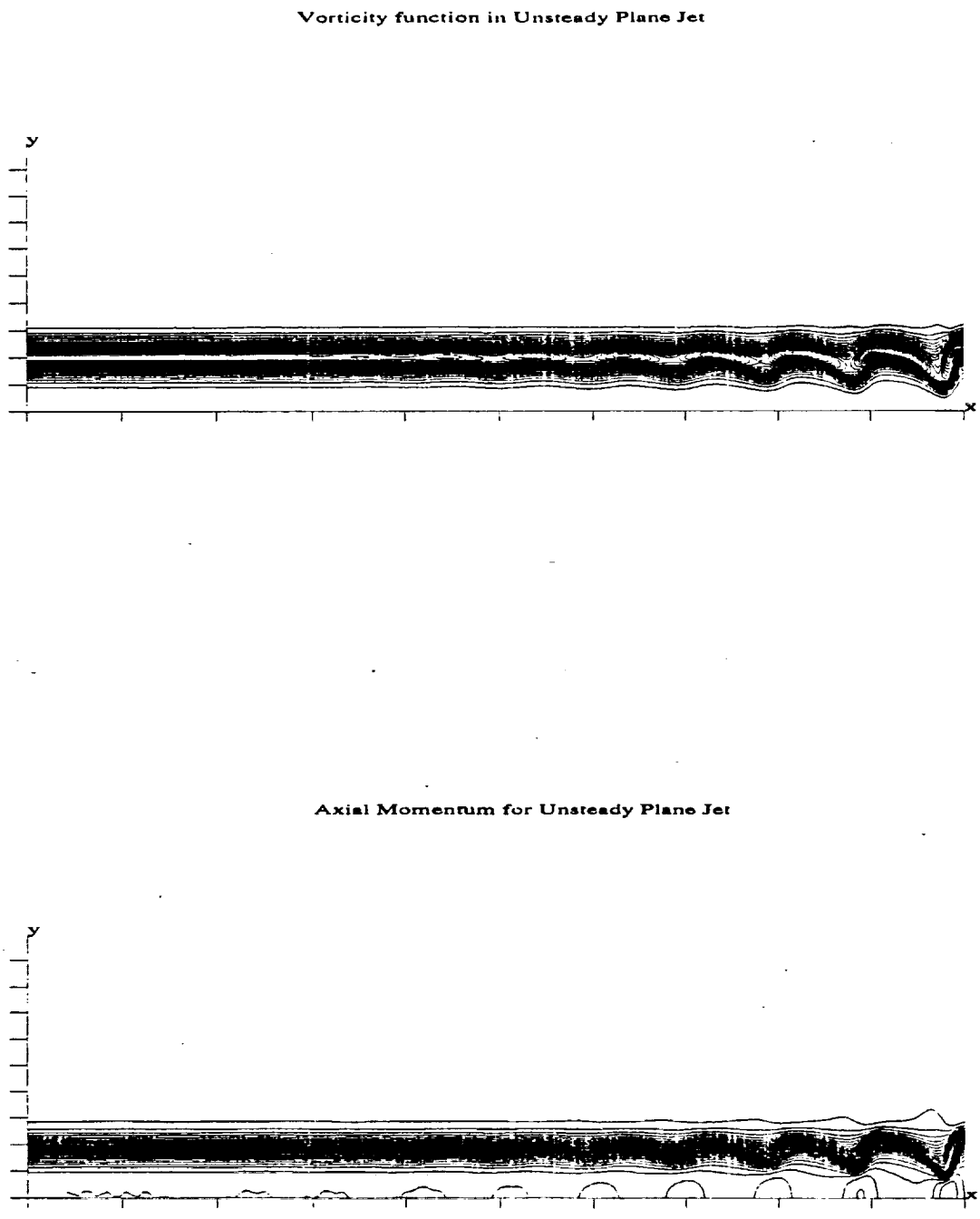

Figure 4: Contour Plots for Unsteady Plane Jet

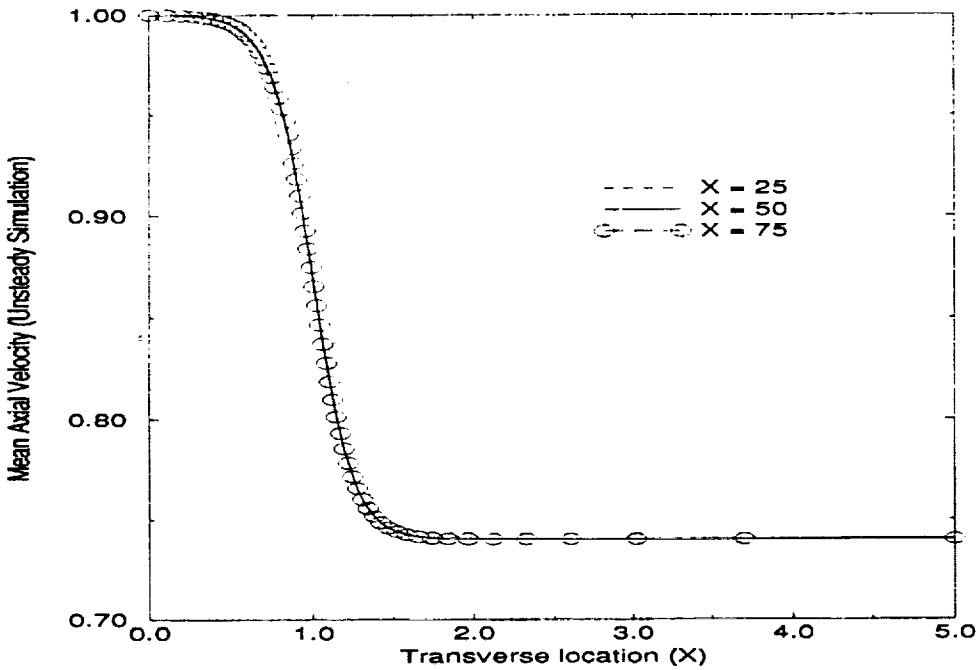

Figure 5: Mean Axial velocity in Unsteady Plane Jet

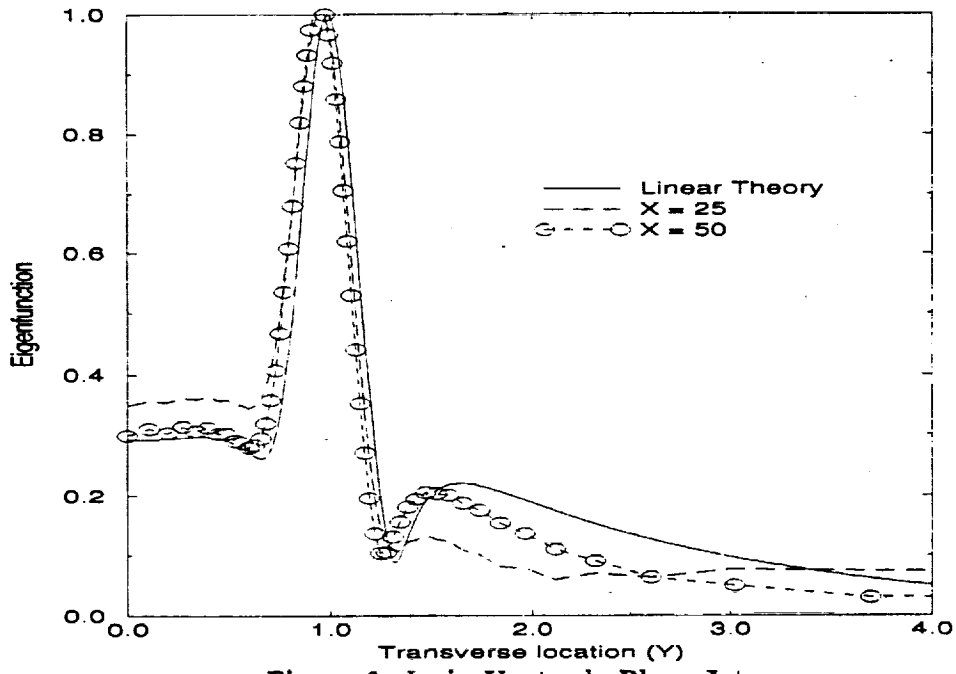

Figure 6: Φ_ω in Unsteady Plane Jet

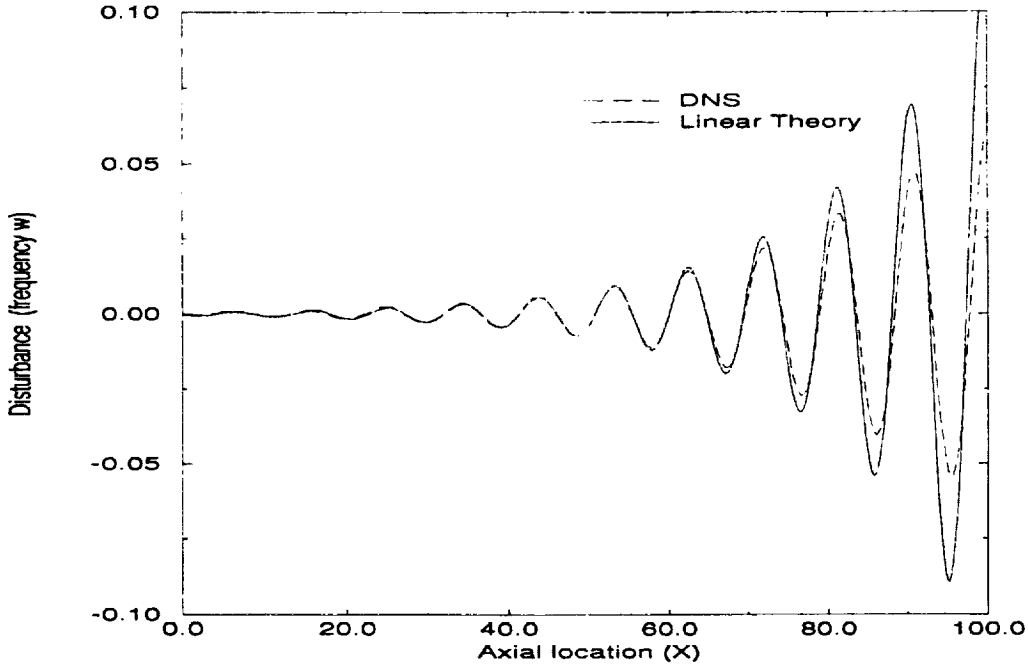

Figure 7: Disturbance growth in unsteady Plane Jet at y=1

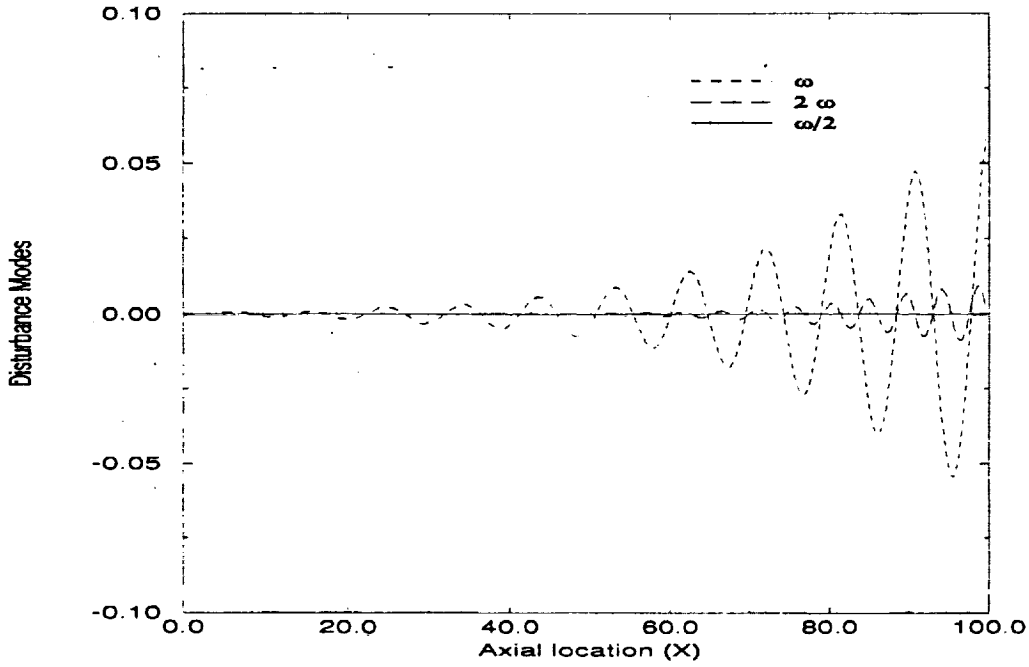

Figure 8: Excitation of disturbance modes in Plane Jetat y=1

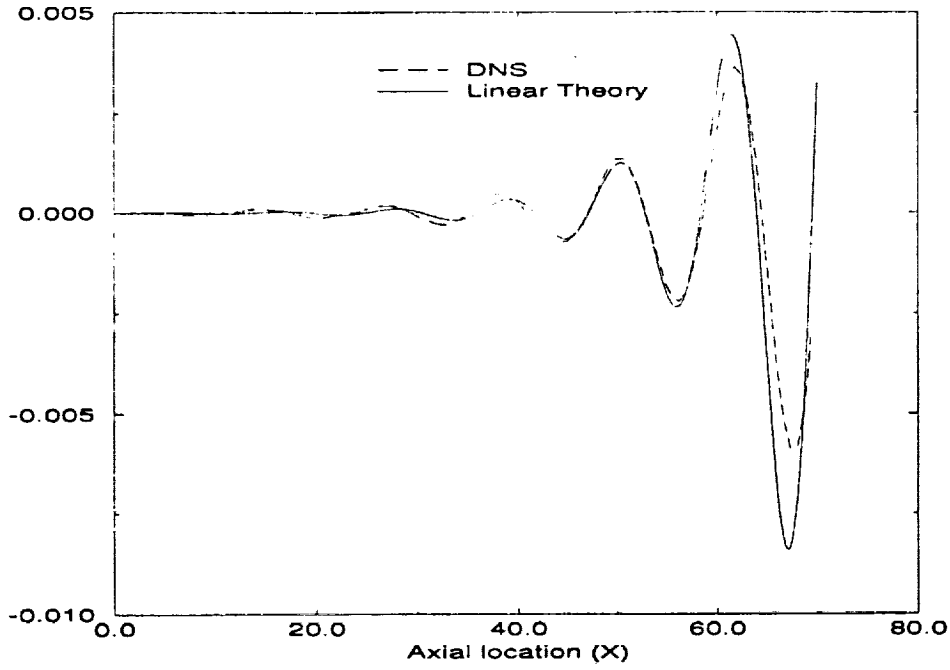

Figure 9: Disturbance growth in unsteady Plane Jet at y=1

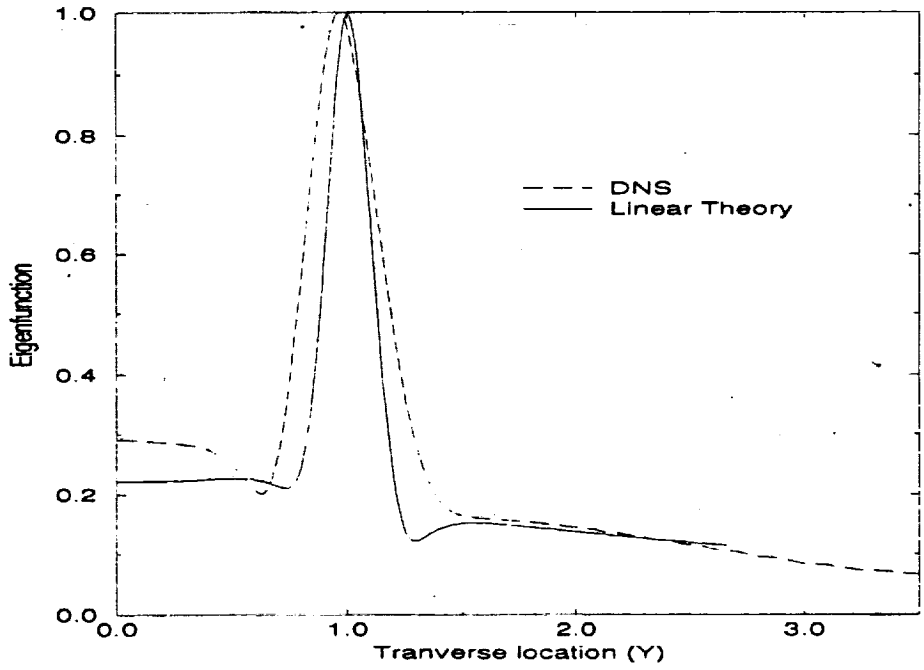

Figure 9: Φ_ω in Unsteady Plane Jet at x=22.6

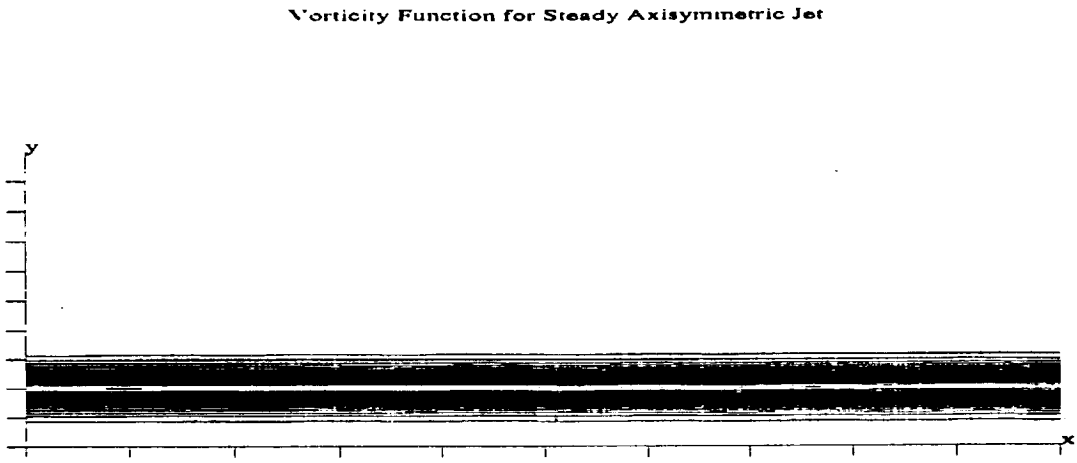

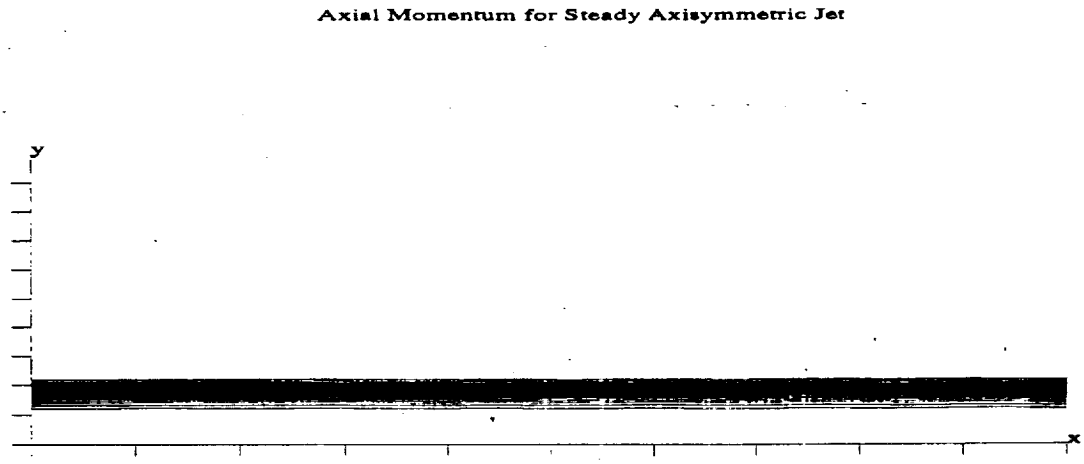

Figure 11: Contour plots for Steady Axisymmetric Jet

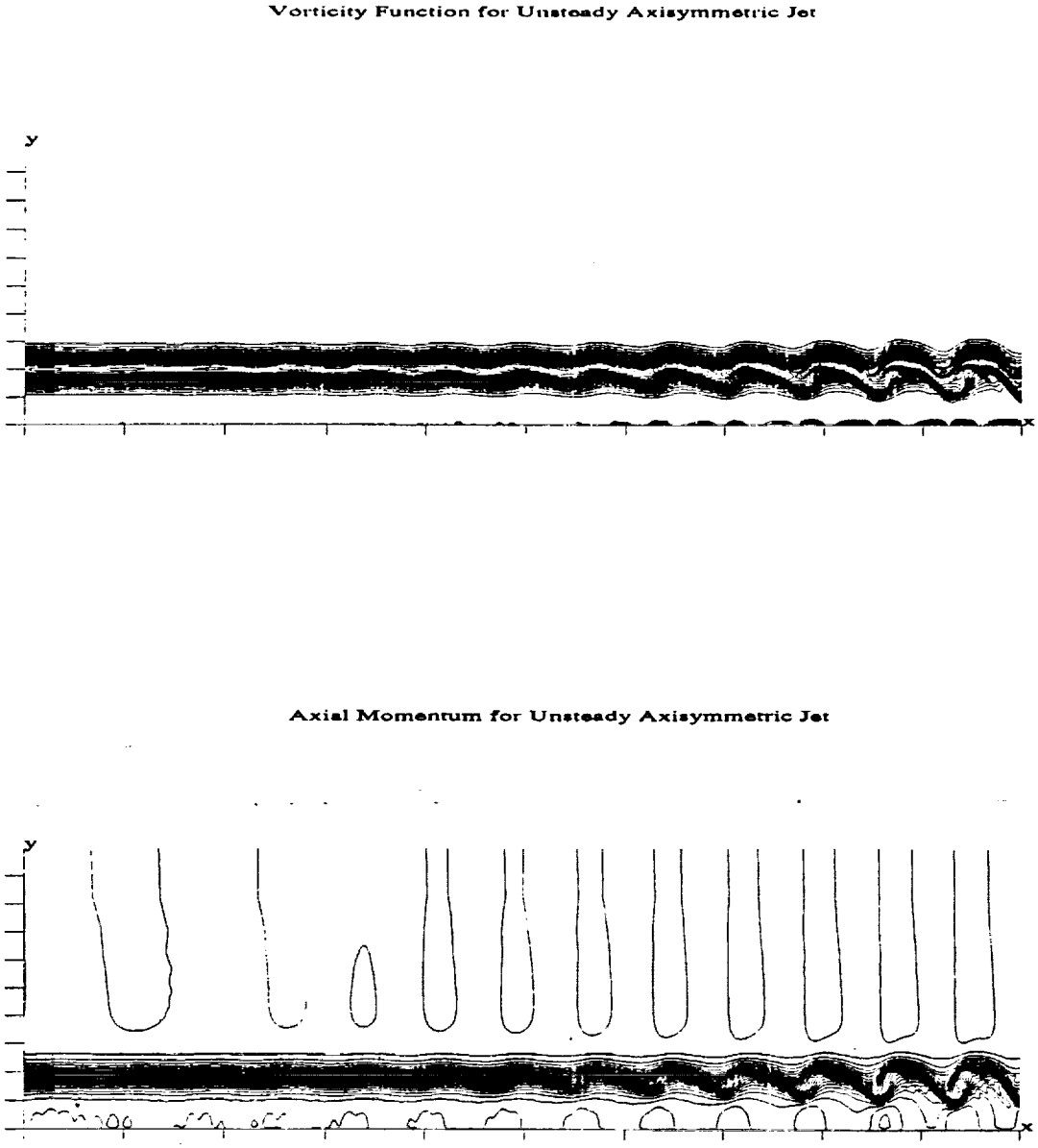

Figure 12: Contour plots for Unsteady Axisymmetric Jet

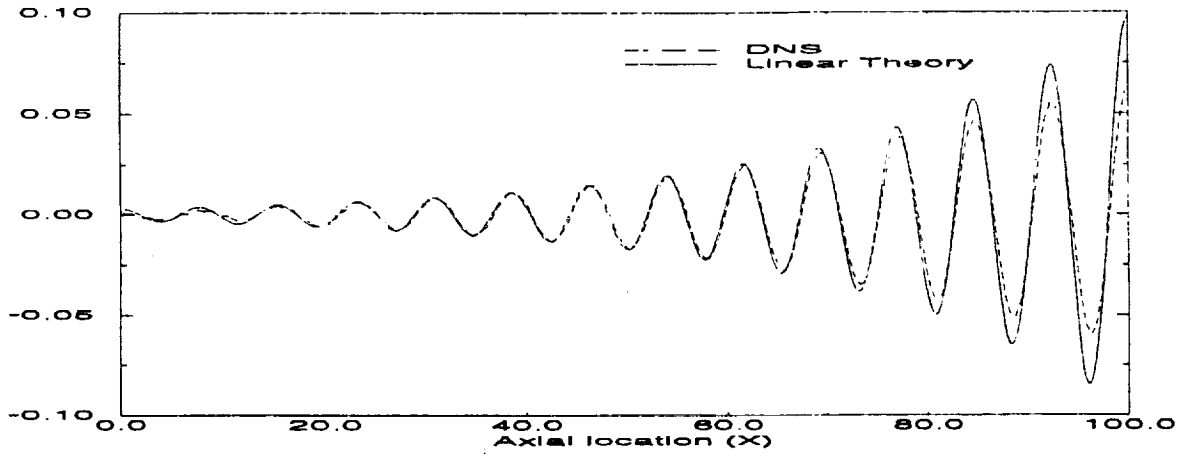

Figure 13: Disturbance growth in unsteady Axisymmetric Jet at r=1

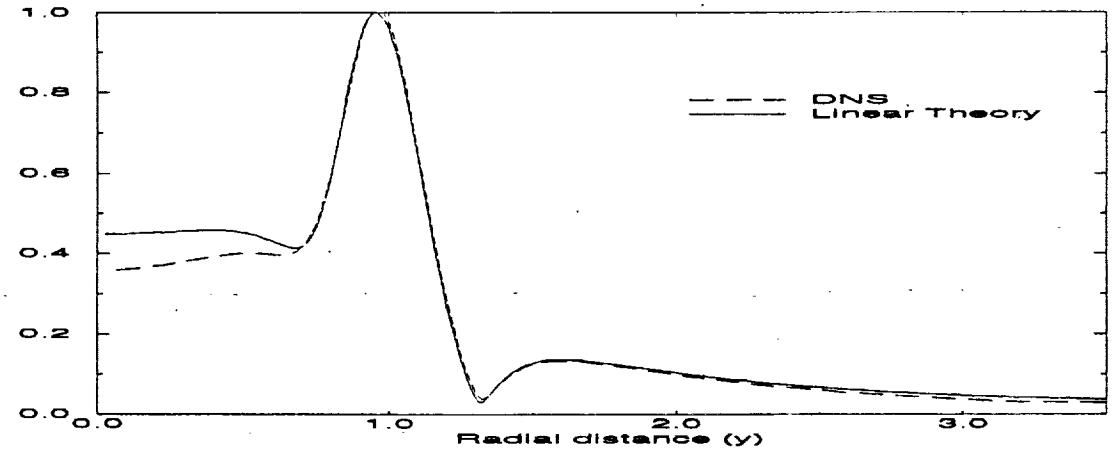

Figure 14: Φ_ω in unsteady Axisymmetric Jet at x=50

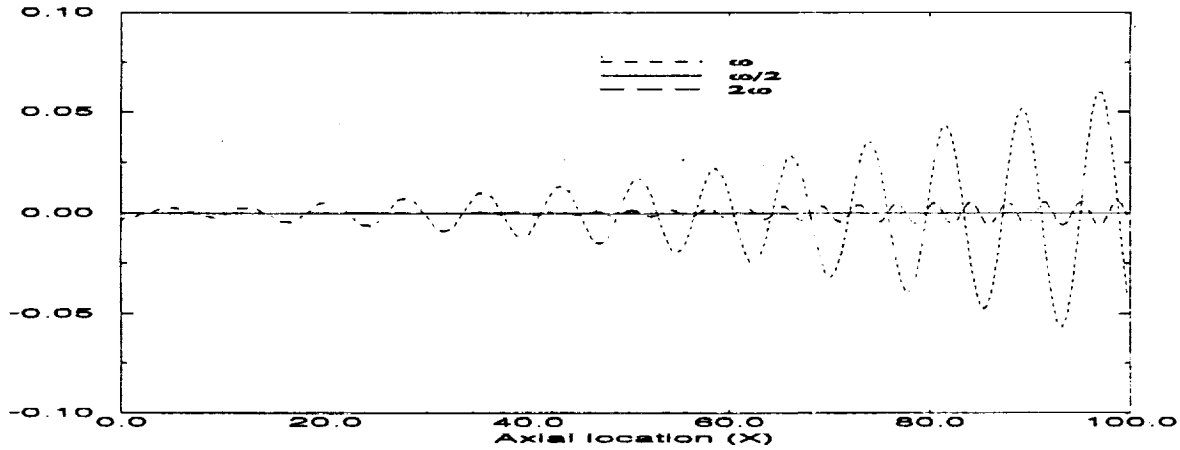

Figure 15: Excitation of disturbance modes in Axisymmetric Jet at r=1

REPORT DOCUMENTATION PAGE

Form Approved
OMB No. 0704-0188

1. AGENCY USE ONLY (Leave blank)	2. REPORT DATE	3. REPORT TYPE AND DATES COVERED
	January 1993	Technical Memorandum

4. TITLE AND SUBTITLE

Numerical Simulation of a High Mach Number Jet

5. FUNDING NUMBERS

WU-505-62-21

6. AUTHOR(S)

Ehtesham Hayder, Eli Turkel, and Reda R. Mankbadi

7. PERFORMING ORGANIZATION NAME(S) AND ADDRESS(ES)

National Aeronautics and Space Administration
Lewis Research Center
Cleveland, Ohio 44135-3191

8. PERFORMING ORGANIZATION REPORT NUMBER

E-7509

9. SPONSORING/MONITORING AGENCY NAMES(S) AND ADDRESS(ES)

National Aeronautics and Space Administration
Washington, D.C. 20546-0001

10. SPONSORING/MONITORING AGENCY REPORT NUMBER

NASA TM-105985

11. SUPPLEMENTARY NOTES

Prepared for the 31st Aerospace Sciences Meeting and Exhibit sponsored by the American Institute of Aeronautics and Astronautics, Reno, Nevada, January 11-14, 1993. M. Ehtesham Hayder and Eli Turke, Institute for Computational Mechanics in Propulsion, NASA Lewis Research Center, Cleveland, Ohio 44135 and Reda R. Mankbadi, NASA Lewis Research Center, Cleveland, Ohio. Responsible person, R. Mankbadi, (216) 433-8569.

12a. DISTRIBUTION/AVAILABILITY STATEMENT

Unclassified - Unlimited
Subject Category 34

12b. DISTRIBUTION CODE

13. ABSTRACT *(Maximum 200 words)*

The recent efforts to develop accurate numerical schemes for transition and turbulent flows are motivated, among other factors, by the need for accurate prediction of flow noise. The success of developing high speed civil transport plane (HSCT) is contingent upon our understanding and suppression of the jet exhaust noise. The radiated sound can be directly obtained by solving the full (time-dependent) compressible Navier-Stokes equations. However, this requires computational storage that is beyond currently available machines. This difficulty can be overcome by limiting the solution domain to the near field where the jet is nonlinear and then use acoustic analogy (e.g., Lighthill[1]) to relate the far-field noise to the near-field sources. The later requires obtaining the time-dependent flow field. The other difficulty in aeroacoustics computations is that at high Reynolds numbers the turbulent flow has a large range of scales. Direct numerical simulations (DNS) cannot obtain all the scales of motion at high Reynolds number of technological interest. However, it is believed that the large scale structure is more efficient than the small-scale structure in radiating noise (see, e.g., Bishop et. al[2], Crington[3], Goldstein[4], Hussain[5,6], Kibens[7], Liu[8,9], Mankabadi and Liu[10], Mankabadi[11,12], Mollo-Christensen[13], and Zaman[14,15]). Thus, one can model the small scales and calculate the acoustically active scales. The large scale structure in the noise-producing initial region of the jet can be viewed as a wavelike nature, the net radiated sound is the net cancellation after integration over space. As such, aeroacoustics computations are highly sensitive to errors in computing the sound sources. It is therefore essential to use a high-order numerical scheme to predict the flow field. The present paper presents the first step in a ongoing effort to predict jet noise. The emphasis here is in accurate prediction of the unsteady flow field. We solve the full time-dependent Navier-Stokes equations by a high order finite difference method. Time accurate spatial simulations of both plane and axisymmetric jet are presented. Jet Mach numbers of 1.5 and 2.1 are considered. Reynolds number in the simulations was about a million. Our numerical model is based on the 2-4 scheme by Gottlieb & Turkel[16,17]. Bayliss et al.[18] applied the 2-4 scheme in boundary layer computations. This scheme was also used by Ragab and Sheen[19] to study the nonlinear development of supersonic instability waves in a mixing layer. In this study, we present two dimensional direct simulation results for both plane and axisymmetric jets. These results are compared with linear theory predictions. These computations were made for near nozzle exit region and velocity in spanwise/azimuthal direction was assumed to be zero. Computational domain of the present study is shown in Figure 1.

14. SUBJECT TERMS

Direct numerical simulation; Plane jet; Axisymmetric jet;
Nonreflecting boundary condition

15. NUMBER OF PAGES

16

16. PRICE CODE

A03

17. SECURITY CLASSIFICATION OF REPORT	18. SECURITY CLASSIFICATION OF THIS PAGE	19. SECURITY CLASSIFICATION OF ABSTRACT	20. LIMITATION OF ABSTRACT
Unclassified	Unclassified	Unclassified	